STABILIZATION OF ALLUVIAL CHANNELS

by

N. G. Bhowmik
D. B. Simons

June 30, 1969

COLORADO WATER RESOURCES

RESEARCH INSTITUTE

Colorado State University
Fort Collins, Colorado

Completion Report No. 6

STABILIZATION OF ALLUVIAL CHANNELS

Partial Completion Report
OWRR Project A-002-COLO

TITLE: SURFACE WATER

June 30, 1969

by

N. G. Bhomik and D. B. Simons
Department of Civil Engineering
Colorado State University

submitted to

Office of Water Resources Research
U. S. Department of Interior
Washington, D. C.

Colorado Water Resources Research Institute
Colorado State University
Fort Collins, Colorado

Norman A. Evans, Director

ABSTRACT

STABILIZATION OF ALLUVIAL CHANNELS

Flow dynamics and the effects of turbulent fluctuations of velocity, drag forces, lift forces, waves and secondary circulations on the stability of riprap particles forming the perimeter of stable alluvial channels were studied. A field study was made of three channels successfully stabilized with gravel riprap. Additional available existing data on initiation of motion and on stable channels formed in coarse materials were gathered and analyzed to explain the flow dynamics and to outline a design procedure for canal stabilization. Necessary relationships were developed to facilitate the design of stable channels formed in coarse alluvial materials.

A design procedure valid for both the straight reaches and the bends to stabilize alluvial channels is presented.

INTRODUCTION

Hydraulics and particularly the design and stabilization of open channels is rather a complex problem. This has long been recognized and much work has been done. But still engineers supplement the analytical approach with their practical knowledge in order to design. Analytical methods for open channel flow lag behind those for close conduit flow, due to the presence of interrelated variables in open channel flow. Change in cross-sectional areas of conveyance systems at different locations, presence of curves and hydraulic structures, undulations on the bed and sides, and small deformations on the channel alignment make the open channel flow non-uniform.

The Problem

Stability of alluvial channels with a special reference to side slopes is very important for the design of stable channels. In some instances the banks and beds of such streams or canals must be stabilized with rip-rap materials. This is necessary because of the design section's inability to carry the design discharge without excessive erosion. Downstream from hydraulic structures, excessive turbulence makes the whole section unstable and the particles are sheared and lifted from the bed and sides. In some instances, inflow makes the side or bed material of alluvial channels practically float, decreasing greatly its resistance to movement; in some instances, wind-generated waves can erode the upper part of the embankment, inducing slip or sloughing failure.

For the study reported here, it was decided to use new and existing field and laboratory data to outline a design criteria valid for stabilizing both straight reaches and bends of alluvial channels.

-1-

Colorado State University Data

Data for this study were collected from the Interstate and Fort Laramie Canals of Wyoming, South Boulder Creek of Colorado, the Charles Hansen Canal near Fort Collins, Colorado, and in the Engineering Research Center Hydraulics Laboratory at Colorado State University.

Data Taken from Other Sources

Other data utilized in this study were taken from: U. S. Waterways Experiment Station, Paper No. 17 (31); Ho and Tu (18); Kalinske (14); Lane and Carlson (16); Punjab Canal Data (21); Journal of Central Board of Irrigation, India (29); Simons and Bender (27); Rolf Kellerhals (15); Urbonas (34); R. S. McQuivey (19); and Colorado State University Stabilization Study (8).

Factors and Variables Affecting Stable Channels in General

The major factors that affect the stable channels are as follows: turbulence; pressure and velocity fluctuations adjacent to and within the bed; drag force; lift force; waves; seepage forces; secondary circulation; shape of the cross section and the reach; vegetation; berms; seasonal variation of roughness; method of operation; bank and bed materials and problem of stabilization; properties of individual particles: shape factor; standard deviation and gradation; fall velocity; and sediment concentration. The important variables are discharge, slope, depth, width, temperature, etc. These factors have been discussed in detail by Simons (27) and Bhowmik (3).

Equations and Relations Essential to Channel Stabilization

Because of the imposed restriction on the length of the paper only those relations and equations used in the proposed design procedure are listed. For a detailed derivation of the equations and a discussion of the figures the reader must refer to reference (3) by the writers.

EQUATIONS

Superelevation--Curvature of the stream lines associated with the centrifugal forces acting on the flow results in a transverse inclination of the free surface. This causes an increase in depth of water at the outer bank and a corresponding decrease of depth at the inner bank. The magnitude of this superelevation can be computed from the relation (3)

$$\Delta Z = \frac{\overline{Vmax}^2}{2g} \left[2 - \left(\frac{r_i}{r_c} \right)^2 - \left(\frac{r_c}{r_o} \right)^2 \right] \tag{1}$$

Secondary Circulation--Secondary circulation is an inevitable result of the unbalanced centrifugal force. The secondary flow causes a vertical velocity component which acts downward on the outside of the bend and it contributes to the unstability of the riprap particles there. The strength of this flow is expressed by the angle α_1 , between the direction of flow near the bed or sides of the channel to the axis of the channel. Rozovskii (23) reported the empirical relation

$$\tan \alpha_1 = 11 \frac{Dmax}{r_c} \tag{2}$$

which was confirmed by Prus-Chacinski (20) to be applicable to both natural and artificial channels.

Non-erosive Velocity in Bends--Rozovskii (23) presented an approximate solution to determine the non-erosive velocities in bends with a width-depth ratio $W_T/D_b > 8$. He proposed a coefficient of reduction of the non-erosive velocity in the bend

$$K' = K_1 K_2 K_3 K_4 \tag{3}$$

where K_1 reflects the increase in maximum velocity, K_2 accounts for the lateral displacement of the maximum velocity, K_3 accounts for the transverse circulation and its effect on bank slope and K_4 corrects for the increase in bottom velocity. The non-erosive velocities in the bend are determined using Figure 14 and the following relations:

$$\Delta' = 0.42 \; \Delta^0 \; \frac{Dmax}{W_T} \; \frac{\sqrt{g}}{C} \tag{4}$$

where Δ^0 is the total deflection angle of the bend, and

$$K_1 = \frac{1}{1 + \Delta V'max} \tag{5}$$

where $\Delta V'max$ is the ratio of average velocity, V, in any vertical to the maximum velocity $Vmax$ in the straight reach

$$K_2 = \left(\frac{D}{Dmax} \right)^{1/6} \tag{6}$$

5) K_3 is computed from

$$K_3 = \left[\left(\frac{Cot^2 \; \alpha - Cot^2 \; \phi \; Cos^2 \; \alpha_1}{1 + Cot^2 \; \alpha} \right)^{\frac{1}{2}} - \frac{Cot \; \phi \; Sin \; \alpha_1}{(1 + Cot^2 \; \phi)^{\frac{1}{2}}} \right]^{\frac{1}{2}} \tag{7}$$

Then K' can be computed from equation 3 assuming $K_4 = 1$. In a straight channel one can assume that

$$Vmax = 1.06 \; \overline{V} \tag{8}$$

Lift Forces--The deflection of the stream lines around the particles decreases the spacing between them, increases the velocity and decreases the hydrostatic pressure over the top of the particles. The lift force is

- 4 -

the resultant of the pressure differences exerted on the surface of the particle and is normally directed upward. To consider the effect of the lift, a lift force factor $\frac{1}{\psi}$ was derived (3) modifying the relationship proposed by Thomson (30) with a special reference of the work performed by Leliavsky (17), Chang (7), Einstein and El-Sami (11), Bakhmeteff (2), Einstein (10), a recent study by Urbonas (34) at Colorado State University and others. This equation states that

$$\frac{1}{\psi} = \frac{V_b^2}{(S_s - 1) \, g \, d_{50}} \left(\frac{\rho_f}{\rho_s}\right) \left(\frac{d_{85}}{d_{50}}\right)^3 \tag{9}$$

If one can approximate the ratio d_{85}/d_{50} the value of d_{50} can be estimated.

Waves

Wind waves are usually defined by their heights, length, and periods. When waves move over the surface of water, only the form and energy of the waves move forward. In deep water, an oscillatory orbital motion of the water particles is caused by the waves, whereas in shallow water, the orbital movement becomes flattened and at the bottom becomes merely horizontal oscillations to and fro as the wave form passes. In shallow flows wind waves may exert a significant shear stress on the bed.

The height, length and period of wind waves are determined by the fetch, speed of the wind, and the length of time that the wind blows. Some research workers (22) studied the magnitude of shear stress on the water air interface due to wind blown waves, and there are several empirical relations between wind velocity and surface shear stress, mostly based on laboratory and some field investigations.

Utilizing research completed by Osvald Sibul (25), the Sverdreys-Mund and Bretschneider relation (5), the work done on effective fetch length by Saville, Jr. (24), the writers (3), suggest the relation

$$gH_s/V_{we}^2 = 3.23 \times 10^{-3} (g F_e/V_{we}^2)^{0.435} \tag{10}$$

In this relation

$$V_{wc} = V_w \cos ⊕ \pm \overline{V}$$

and

$$F_e = 1.17 F^{1/3} W_T^{2/3}$$

Knowing wind velocity and direction, fetch length and width, and the flow velocity, the significant wave height in an open channel can be estimated using equation (10).

Modification of Bottom Shear Stress Due to Waves--Wind-generated waves modify the velocity distribution in open channels and may cause an additional shear stress on the bed and banks of the channel. Using the results of studies by Bretschneider (5), Bijkar (4) and the writers the maximum bottom velocity caused by a wave is

$$V_{wm} = \frac{\pi H_s}{T} \frac{1}{\sinh \frac{2\pi D}{L}} \tag{11}$$

and the ratio τ_t/τ_o is

$$\frac{\tau_t}{\tau_o} = 1 + 0.0324 \left[c/\sqrt{g} \frac{u_b}{V} \right]^2 + 0.36 \frac{u_b}{V} c/\sqrt{g} \tag{12}$$

Knowing $\overline{V}$; $C/\sqrt{g}$; D , significant wave height, H_s ; wave period, T ; and wave length, L ; and replacing u_b , the bottom velocity by V_{wm} from equation 11 the maximum and mean increase in bottom shear stress due to waves are given by equations 12 and 13.

$$\frac{\tau_t}{\tau_o} = 1 + 0.0162 \left[C/\sqrt{g} \; \frac{u_b}{\overline{V}} \right]^2 \tag{13}$$

This is in addition to the shear stresses associated with uniform flow.

Stability of Riprap Particles--The stability of riprap particles is affected by all of the foregoing forces caused by flowing water acting on the exposed particles.

Sides of Straight Reaches

Referring to the following figure which considers the sides of straight reaches of channels and taking moment about the point of particle support

<u>Figure</u>   (see attached page)

$$\tan\phi = \frac{R_e}{N_F} = \frac{[(F_D + F_P + F_I)^2 + (F_B \; \mathrm{Sin}\alpha \mp f_s \; \mathrm{Cos} \; \chi)^2]^{1/2}}{(F_B \; \mathrm{Cos}\alpha - F_L \mp f_s \; \mathrm{Sin} \; \chi)} \tag{14}$$

In order to solve this complicated equation, the following assumptions are made:

1. At high IR , the coefficient of drag, C_D , can be assumed to be constant and as such drag and lift forces predominate, (9,31).

2. Lift and drag predominates at high IR , hence, it can be assumed that all accelerating forces are negligible in comparison to gravity, drag, and lift forces.
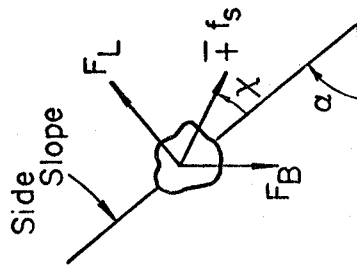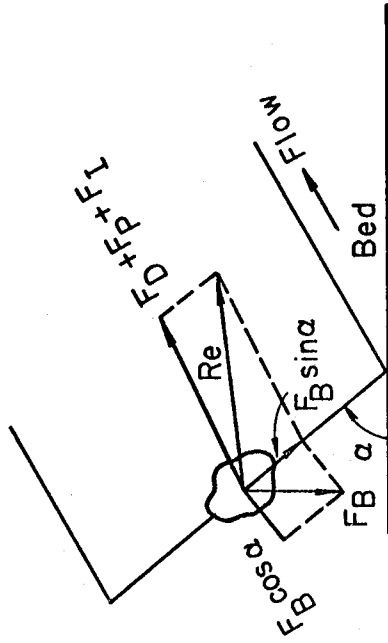
3. Seepage forces are neglected.

4. Based upon work on spheres, it can be assumed that the coefficient of lift, C_L, is a function of coefficient of drag, C_D, (9,31) and

$$C_L = 0.85 \ C_D$$

5. The effective projected area of the particles for both lift and drag forces are the same.

6. For high $\mathbb{R}$, C_D can be approximated to be equal to 0.9. Although Eagleson and Dean (9) and Torum (31) assumed C_D to be equal to 1.0.

7. The mass density of the fluid ρ_f is assumed to be equal to 1.94 lbs - $\sec^2/ft^4$ and the specific weight of water γ is equal to 62.4 lbs - per cubic foot.

With these assumptions equation 14 becomes

$$K_7^2/K_8 = 1 \tag{15}$$

where,

$$K_7 = [(\gamma_s - \gamma) \cos\alpha - 0.743 \ V_b^2 n] \tan\phi \tag{16}$$

$$K_8 = [0.76 \ (V_b^2 n)^2 + \{(\gamma_s - \gamma) \sin\alpha \}^2 \ ]^{\frac{1}{2}} \tag{17}$$

$$n = \text{stability coefficient} = C_2/C_1 d_s$$

Equation 17 is in the form to be utilized for the stability analysis of riprap particles on the side slopes of straight reaches.

Concave Side Slopes of Bends--The riprap particles on the concave side slopes of bends near the exit from the bend are most susceptible to

- 9 -

erosion due to increased flow velocity and transverse circulation. Effects due to secondary circulation can be dealt with by utilizing the concept that the direction of velocity vector acting on the particle is deflected by an angle α_1 in the downward direction, increasing the instability of the particle. Referring to the following figure

<u>Figure</u>   (see attached page)

with ϕ as the submerged angle of repose as before and taking moments about the point of support,
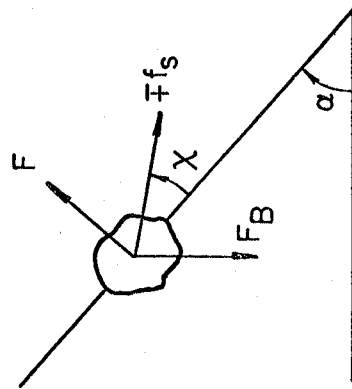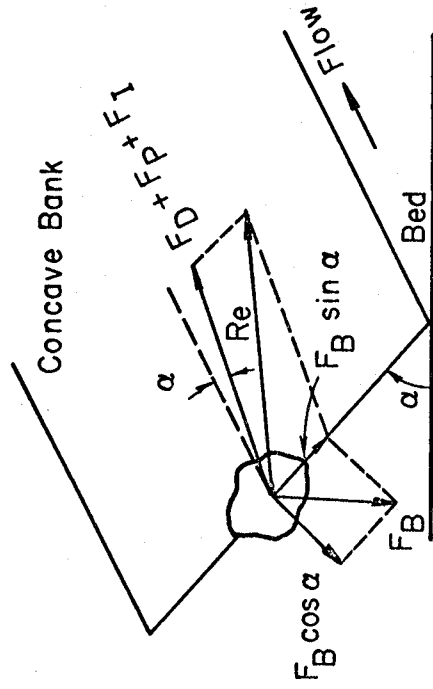
$$\tan\phi = \frac{R_e}{N_F} \tag{18}$$

Using the same assumptions as in the preceding section, equation 18 becomes

$$K_7 = [K_8 + 1.74 \ V_{b_n}^2 (\gamma_s - \gamma) \ \mathrm{Sin}\alpha_1 \ \mathrm{Sin} \ \alpha]^{\frac{1}{2}} \tag{19}$$

Whenever $\alpha_1 = 0$, equation 19 is exactly the same as 15. The numerical value of α_1 is required to solve equation 19. Brooks (6) suggested that $\alpha_1 = 20^{\circ}$ and for small values of α_1, $\tan\alpha_1 = \mathrm{Sin}\alpha_1$. Then substituting equation 2 in equation 19 the final expression is

$$K_7 = [K_8 + 19.12 \ V_{b_n}^2 (\gamma_s - \gamma) \ \frac{D_{max}}{r_c} \ \mathrm{Sin}\alpha \ ]^{\frac{1}{2}} \tag{20}$$

and K_7 and K_8 were previously defined.

Concave Bank

$F_D + F_P + F_1$

Flow

α

Re

$F_B \sin \alpha$

Bed

α

$F_B \cos \alpha$

F_B

$\mp f_s$

F

χ

F_B

α

The Bed of a Straight Reach--Referring to the following figure, with ϕ as the submerged angle of repose and taking moments about the point of support

<u>Figure</u>   (see attached page)

$$\tan\phi = \frac{R_e}{N_F} \tag{21}$$

Making the same assumptions as on the preceding paragraphs, equation 21 reduces to

$$\frac{1.146\left[(\gamma_s-\gamma)\ \tan\phi\ \cos\alpha' + (\gamma_s-\gamma)\ \sin\alpha'\right]}{V_b^2\ (1 + 0.85\ \tan\phi)} = \frac{C_2}{C_1 d_s} = \eta \tag{22}$$

When the invert slope α' is very small, then $\cos\alpha' = 1.0$, $\sin\alpha' \approx 0$ and equation 22 reduces to

$$\frac{1.146\ (\gamma_s-\gamma)\ \tan\phi}{V_b^2\ (1 + .85\ \tan\phi)} = \frac{C_2}{C_1 d_s} = \eta \tag{23}$$

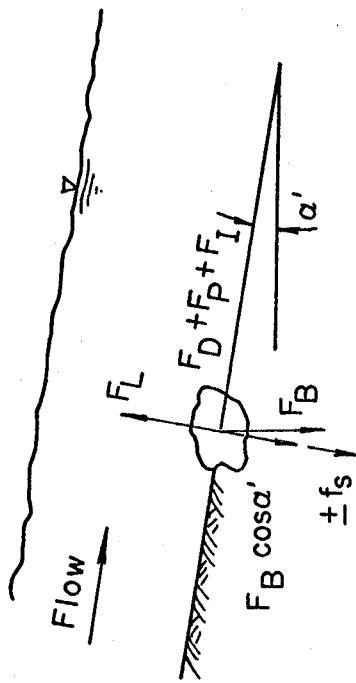This is the equation recommended for stability analysis of irregular shaped particles resting on a bed of negligible slope with no seepage forces acting.

For spherical particles equation 23 reduces to

$$\frac{d\ (\gamma_s-\gamma)\ \tan\phi}{\rho_f\ V_b^2\ (1 + .85\ \tan\phi)} = 3/10$$

or

$$\frac{d\ (\gamma_s-\gamma)}{\tau_0}\ \left(\frac{V_*}{V_b}\right)^2\ \frac{\tan\phi}{(1 + 0.85\ \tan\phi)} = 3/10 \tag{24}$$

- 12 -

The first term on the left-hand side of this equation is the inverse of the Shields parameter which states that $T_c = \dfrac{\tau_o}{(\gamma_s - \gamma) d}$. Iwagaki (13) recommended that $T_c = 0.05$, for armor material and Gessler (12) suggested a limiting value of $T_c = 0.047$.

Straight Reaches, Seepage Forces Negligible--With negligible bed slope, the ratio of the drag forces is given by

$$(F_{DS}/F_{Db})^2 + (F_{DS}/F_{Db}) K_9 (1.7 \, Cos\alpha \, tan\phi) = K_{10} \tag{25}$$

where

$$K_9 = \frac{(1 + 0.85 \, tan\phi)}{(1 - 0.72 \, tan^2\phi)} \tag{26}$$

and

$$K_{10} = \frac{(1 + 0.85 \, tan\phi)^2 \, (Cos^2\alpha \, tan^2\phi - Sin^2\alpha)}{tan^2\phi \, (1 - 0.72 \, tan^2\phi)} \tag{27}$$

These relations are valid for small bed slope. Brooks (6) assumed drag forces are proportional to shear stress

$$F_{DS}/F_{Db} = \tau_s/\tau_o \tag{28}$$

With this assumption equation 25 becomes

$$(\tau_s/\tau_o)^2 + (\tau_s/\tau_o) K_9 (1.7 \, Cos\alpha \, tan\phi) = K_{10} \tag{29}$$

When seepage forces are not negligible, the equation is complicated.

Resistance Coefficients--Correct determination of the average shear stress depends greatly on the accurate measurement of energy slope. This can be avoided to some extent by relating hydraulic roughness to stable riprap sizes. Figure 12 shows that Manning's roughness factor, is related to the d_{50} size by

$$37.6n = d_{50}^{0.178} \tag{30}$$

The original riprap materials through which the channels were constructed must have originally contained some fine materials which were washed away. Knowing the initial and final bed composition for channels constructed in noncohesive materials, Lane (16) related Manning's roughness factor, n , with the d_{75} size of the initial riprap material

$$39n = d_{75}^{1/6} \quad . \tag{31}$$

It is to be noted that equation 30 relates the stable riprap sizes exposed on the bed after construction and operation of the channel to Manning's n .

Graphical Relations for Design--Based upon theory and laboratory and field experiments, several graphical design relations were developed by Bhowmik (3). Those essential to the suggested design procedure are presented in Appendix A.

Angle of Repose of Non-Cohesive Material--The stability analysis of riprap materials requires knowledge of the angle of repose of riprap particles. Figure 13 provides a relation between angle of repose and the shape and mean diameter of the particles (27).

Relation Between Riprap Materials and Flow Parameters--One of the most important flow parameters determining riprap size is flow velocity. A relation between the average flow velocity and mean particle diameter is given in figure 1.

Channel Geometry--In figures 2, 3, and 4, the relations between top width W_T and discharge Q , average depth $\bar{D}$ and discharge Q ; and the area of water cross-section A and Q , respectively are presented. A wide range of field data were used to establish these relations.

Average Velocity--Two relations based upon work done by Simons and Richardson (26) and Bhowmik (3) are presented. Figure 5 relates a depth correction ΔD and average depth $\overline{D}$. Figure 6 is the accompanying resistance diagram which relates $\Delta D/\overline{D}$, $\mathbb{R} = \dfrac{V_* \overline{D}}{\nu}$ and the Chezy coefficient $C/\sqrt{g}$. The latter relation is analogous to the Moody type pipe resistance diagram.

Average Velocity as a Function of Average Depth $\overline{D}$ and Energy Gradient, Se --Figure 7 relates average velocity, average depth and slope of energy gradient as has been done by Kellerhals (15).

Stability Coefficient--Figure 8 relates the stability coefficient η and the particle Reynolds number. The stability coefficient was computed by equation (23).

Relation Between Average Shear Stress and the d_{85} Size of the Bed Material--Figure 9 relates τ_0 to the d_{85} size of bed material. The average relation between shear stress and the d_{85} size is given by the relation

$$\tau_0 = 0.186 \ d_{85}^{0.78} \tag{32}$$

Turbulent Intensity--Figure 10 relates the relative intensity of turbulence $\dfrac{\sigma}{\overline{V}}$ to the relative depth y/D. The relations are based upon data from the Mississippi River, Kalinske (14), and a flume study by McQuivey (19).

Lift Force--Figure 11 relates the lift force factor $\dfrac{1}{\psi}$ to the flow Reynolds number where the Reynolds number is a function of bottom velocity or flow velocity near the particles. Equation (9) gives the relation for $\dfrac{1}{\psi}$.

Manning's n as a Function of Particle Size--Figure 12 shows that Manning's roughness factor is related to d_{50} size by $37.6n = d_{50}^{0.178}$.

Dimensionless Curves to Estimate Bend Effects on Velocity and Stability--Figure 14 gives dimensionless curves to evaluate bend effects on channel stability. These relations were proposed by Rozovskii (23).

Maximum Velocity in the Bends--Figure 15 relates the average velocity to the maximum observed velocity in the bends studied.

Superelevation of the Water Surface--Figure 16 relates the maximum measured superelevation to the superelevation computed by equation 1. The observed values are larger than the computed values.

PROPOSED DESIGN PROCEDURE

Straight Reaches

With knowledge of the design discharge, Q , and the material type through which the channel is to be constructed, the design steps to be followed are:

1) From a knowledge of the material type, estimate the allowable average velocity, $\overline{V}$, from Figure 1 using the "design curve". Most of the data relating mean particle size and average flow velocity from existing stable channels plots to the left of this design curve (Figure 1). Therefore, the average velocity estimated from this line for a particular mean particle size should be safe from erosion.

2) Select water surface width, W_T , from Figure 2 and average depth, $\overline{D}$, from Figure 3 ($W_T/\overline{D} \geq 15$). The product of the values of W_T and $\overline{D}$

thus selected should be consistent with the flow area, A , as shown in Figure 4 ($W_T/\overline{D} \geq 15$). Flow velocity, $\overline{V}$, is equal to Q/A and this is approximately equal to the velocity selected in step 1. For any discrepancy between these two velocities repeat step 2 changing W_T and $\overline{D}$ until the velocities are equal.

3) Determine the value of the slope, S , to obtain the selected value of $\overline{V}$ in step 1 as follows:

a) Estimate a value of S .

b) With known $\overline{D}$ estimate the value of ΔD from Figure 5.

c) From the anticipated water temperature estimate the value of kinematic viscosity, ν , and then compute: relative roughness, $\Delta D/\overline{D}$; shear velocity, $V_* = \sqrt{g\overline{D}S}$ and shear Reynolds number, $\mathbb{R}_* = V_*\overline{D}/\nu$.

d) Enter the $C/\sqrt{g}$, $\overline{\mathbb{R}}_*$ relation (Figure 6) in which $\Delta D/\overline{D}$ is the third variable and read the value of $C/\sqrt{g}$ corresponding to the values of $\overline{\mathbb{R}}_*$ and the relative roughness, $\Delta D/\overline{D}$.

e) Compute the average velocity from the relation

$$\overline{V} = C/\sqrt{g} \; V_*$$

(33)

f) Check the computed average velocity obtained in step 3-e with the velocity estimated in step 1; if both the velocities are about the same, the design so far is all right, otherwise select a new value of S and repeat step 3. A quick check on the estimated values of $\overline{D}$, V and S can be made with the aid of Figure 7 and for significant differences, recheck the estimation of $\overline{V}$ in step 1 and the arithmetic in step 2 and step 3.

4) With known $\bar{V}$, S and ν , compute the stability coefficient, n for the bed by equation 22 and estimate the required d_{50} for the bed material from Figure 8. The value of V_b can be taken as equal to 80 percent of $\bar{V}$ however this value of V_b should be increased by 50 percent to account for the turbulent fluctuations of velocity before applying the coefficient.

5) Check the estimated value of d_{50} in step 4 with the mean diameter of the locally available riprap. If the d_{50} size estimated in step 4 is larger than the mean diameter of the bed material or the riprap particles available locally, repeat step 1 through step 5, reducing $\bar{V}$ and S , changing W_T and $\bar{D}$ so their values are consistent with Q and $\bar{V}$.

6) Compute the shear stress on the bed, $\tau_o = 1.5\gamma\bar{D}S$ and estimate the d_{85} size of the bed material from Figure 9. The shear stress on the bed has been increased by 50 percent to account for the turbulent fluctuations of shear stress associated with turbulent fluctuations of flow velocity. Assuming the turbulent fluctuations of dimensionless shear stress, $\tau/\bar{\tau}_o$ follows a Gaussian normal distribution, Gessler (12) has found the value of the standard deviation, σ' , to be equal to 0.57. Increasing the average shear stress by 50 percent (approximately equal to one standard deviation) was mainly based on the above conclusion and the magnitudes of turbulent velocity fluctuations as shown in Figure 10.

7) With known, V_b , d_{50} , d_{85} and ν , compute the lift force factor $1/\psi$ by equation 9 and check the stability of riprap against lifting using Figure 11. If the computed point falls in the unstable portion of the plot (Figure 11) repeat steps 1 through 7.

8) Estimate the d_{75} size of riprap by combining Lane's (16) equation relating Manning's n and d_{75} size given by equation (31), and equation (30) relating Manning's n and d_{50} size obtained from Figure 12 to obtain

$$d_{75}^{1/6} = 1.04 \, d_{50}^{0.178}$$

9) With the known bed material or riprap size, d_{50} (step 4), estimate the angle of repose, ϕ , from Figure 13. For stability on the sides their inclination, α , should be less than the estimated value of ϕ . Selection of the value of $\alpha < \phi$ depends on hydraulic factors, type of riprap, experience and economic considerations.

10) Compute the stability coefficient, η , from equation 15 for the banks and estimate the d_{50} size for banks from Figure 8.

11) Compute the ratio of shear stress, $\tau_s/\tau_0 = E$, by equation 29 and knowing τ_0 , from step 6, find the design shear stress for banks, $\tau_{sd} = \tau_0/E$. Estimate the d_{85} size for bank material from Figure 9, substituting τ_{sd} for τ_0 (Figure 9).

12) Compute $1/\psi$ for the banks by equation (9) and check to make certain the particles will resist the lift forces using Figure 11. If the particles are not safe against lifting, repeat steps 1 through 12.

13) If heavy wave action is anticipated near the banks, check the estimated d_{85} size in step 11 as follows:

a) Compute significant wave height, H_s , by equation (10).

b) Compute u_b by equation (11) with an assumed wave period, T , and wave length, L , for variable depths on the banks up to a maximum of six feet (27).

c) Replace τ_0 in equation (12) by τ_{sd} and compute τ_t/τ_{sd} , where $\tau_t = \tau_0$ + shear stress due to wind-generated waves.

d) With known τ_{sd} from step 11, compute τ_t .

e) Find the d_{85} size of riprap materials from Figure 9, replacing τ_0 in Figure 9 with τ_t obtained in step 13-d. For significant wave activity, the d_{85} size obtained in this step will be greater than the d_{85} size obtained in step 11. But the increase in shear stress due to waves will be largest near the upper portion of the banks, whereas, the maximum shear stress due to uniform flow acts on the banks at a depth about 2/3 D (16) and the magnitude of τ_s decreases toward the upper portion of the banks. Therefore, the larger d_{85} size associated with maximum shear stress (step 11) may compensate for increased shear stress due to waves near the upper portion of the banks. If the difference between the estimated d_{85} sizes in step 11 and step 13-e is significant, use the latter value for the bank material.

14) Freeboard: It must be remembered that proper selection of freeboard depends on hydraulic condition and the judgment and experience of the engineers. The freeboard is generally fixed by channel size and location, storm water inflow, water table fluctuations, wind waves, soil characteristics, percolation gradients, operating road requirements and availability of fill materials to build up bank height. The freeboard may be estimated from the relation

$$F_b = H_s + (0.5 \text{ to } 1 \text{ ft})$$

where H_s is the significant wave height from equation (10). However, local conditions may sometimes dictate a higher value of F_b .

Bends

For a bend with $W_T/Dmax \geq 8$, $W_T/r_c < 0.60$ which is flowing at low Froude number (Fr < 0.2), the following procedure can be utilized to find the nonerosive velocities. Use steps 1 through 3 as for straight reaches.

15) Compute the maximum velocity in the bend as follows:

a) Compute Δ' from equation (4). The value of $C/\sqrt{g}$ may be taken from step 3-d.

b) Knowing Δ' enter Figure 14 and read the values for $2X'/W_T$ and $\Delta V'max$. Note that $\Delta' \times 10^2 = 21.0$ represents the maximum bend effects.

c) Using a cross-sectional shape as obtained for straight reaches determine the depth of flow, D, in the vertical with the maximum mean velocity at the end of the bend. Then

d) Compute:

$$K_1 = 1/(1 + \Delta V'max) \tag{5}$$

$$K_2 = (D/Dmax)^{1/6} \tag{6}$$

and $K_3 = E_1^{1/2}$, where E_1 is given by

$$(F_{DS}/F_{Db})^2 + (F_{DS}/F_{Db})\left[\frac{1.7\ Cos\alpha tan^2\phi + 2Sin\alpha Sin\alpha_1}{tan\phi}\right] K_9 = K_{10} \tag{35}$$

and $E_1 = F_{DS}/F_{Db}$.

e) The maximum average velocity in the bend for the bed is equal to the average velocity determined for straight reaches divided by K_1 and K_2, i.e., $V = \overline{V}/K_1K_2$.

- 22 -

f) The maximum average velocity for the concave bank at the end of the bend is equal to the average velocity determined for the straight reach divided by K_1, K_2 and K_3.

16) Compute the stability coefficient, n, for the bed by equation (22) using the maximum average velocity in step 15-e and then estimate the required d_{50} size of the bed material from Figure 8.

17) Compute the stability coefficient, n, for concave banks by equation (20) utilizing the maximum average velocity obtained in step 15-f and α estimated in step 9, then estimate the required d_{50} size of bank material from Figure 8.

18) To estimate the required d_{85} size of the bank material, compute the ratio of $\tau_s/\tau_0 = E_1$ by

$$(\tau_s/\tau_0)^2 + (\tau_s/\tau_0)\left[\frac{1.7\ \cos\alpha\tan^2\phi\ +\ 2\sin\alpha\sin\alpha_1}{\tan\phi}\right] K_9 = K_{10} \qquad (35)$$

and knowing τ_0 from step 6, find the design shear stress for the concave side of the bends, $\tau_{sd} = \tau_0/E_1$. Estimate the d_{85} size from Figure 9 substituting τ_{sd} for τ_0 in Figure 9.

19) Check the stability of particles against lifting as follows:

a) Compute $1/\psi$ by equation (9) for the bed and check the stability of particles against lifting using Figure 11. If the particle is not stable repeat steps 1 through 3 and steps 15, 16 and 19a.

b) Compute $1/\psi$ by equation (9) for the banks and check the stability of particle against lifting using Figure 11. If the particle is not stable repeat steps 1 through 3 and steps 15, 17, 18 and 19b.

20) If heavy wave action is anticipated near the bank, follow step 13 with the following exceptions: replace step 11 mentioned in step 13-d and 13-e by step 18.

21) Estimate the maximum superelevation with the aid of Figure 16 and equation (1).

22) Estimate freeboard by adding the superelevation obtained in step 21 and the significant wave height obtained in step 13-a. This estimated value of freeboard may be modified to suit local requirements.

For a short radius bend ($W/r_c > 0.6$; $W_T/D < 8$) with a large deflection angle, the procedure outlined above can be modified as follows.

The core of the higher velocities is located near the axis of the upstream straight reach for the type of bends mentioned above. These filaments of higher velocities impinge on the concave side of the bends near the downstream part. Thus, the nonerosive velocities for bends with smaller radius and higher deflection angle are less than the nonerosive velocities associated with large radius bends. To account for this increase in velocity the procedure is

23) Replace the coefficient K_1 and K_2 in step 15-d by the following single coefficient

$$K_1 K_2 = K_{12} = \frac{\overline{V}}{1.42 \ \overline{V}} = 0.705 \tag{36}$$

This coefficient was obtained from the results of the present study (Figure 15). As an alternative the California Division of Highways (28) recommends a value of 0.75 for the coefficient K_{12}.

24) All other steps outlined before are the same for this type of bends with the modification mentioned in step 23.

Riprap particles for convex banks of bends may be determined as for banks of straight reaches. Stable rocks used or recommended for concave banks at the exit section of bends may be continued upstream to the beginning of the bends.

SUMMARY AND CONCLUSION

Flow dynamics and the effects of turbulent fluctuations of velocity, drag forces, lift forces, waves and secondary circulations on the stability of riprap particles forming the perimeter of stable alluvial channels were studied. A field study was made of three channels successfully stabilized with gravel riprap. Additional available existing data on initiation of motion and on stable channels formed in coarse materials were gathered and analyzed to explain the flow dynamics and to outline a design procedure for canal stabilization.

An equation based on simple and fundamental physical relations was developed to estimate the stability of riprap particles, considering lifting. This relation, designated by the lift force factor, $\frac{1}{\psi}$ is related to the flow Reynolds number.

Wind-generated surface waves may cause a considerable shear stress due to uniform flow. Equations developed to predict significant wave heights and increased bottom shear stress due to waves for shallow streams with unlimited fetch and width were modified to apply to streams with limited fetch and width so this added force could be considered.

The total resistance to flow is expressed by a single roughness factor called depth correction ΔD and relevant relationships were developed to predict the average velocity in a straight channel.

The discharge, Q, was related to other flow parameters, such as flow area A, water surface width W_T, average depth, and average velocity for channels formed in alluvium ranging in size from fine sand

-26-

to loose rocks.

Stability coefficient, η, was related with the particle Reynolds number. This relation can be utilized to estimate the stable mean riprap size for either the bed or the bank in both straight reaches and bends.

Stable mean bed material size, d_{50}, is related to the average bottom velocity and in some cases with the average velocity.

A design procedure valid for both the straight reaches and the bends to stabilize alluvial channels is presented.

APPENDIX I. - REFERENCES

1. Albertson, M. L., Barton, J. R., and Simons, D. B., 1961, Fluid Mechanics for Engineers, Prentice-Hall, Inc., Englewood Cliffs, N. J., 561 p.

2. Bakhmetelf, B. A., 1962, Advance Computations of Hydraulic Forces, Appendix B, Review of Research on Channel Stabilization of the Mississippi River 1931-1962, by Tiffany, J. B., pp. B1 - B9.

3. Bhowmik, N. G., 1968, The Mechanics of Flow and Stability of Alluvial Channels Formed in Coarse Materials, Ph.D. Dissertation, Colorado State University, Fort Collins, Colorado, 207 p.

4. Bijkar, E. W., 1967, Some Considerations About Scales for Coastal Models with Movable Beds, Publication No. 50, Delft Hydraulics Laboratory, Delft, Netherlands, 142 p.

5. Bretschneider, C. L., 1954, Generation of Wind Waves Over a Shallow Bottom, Beach Erosion Board, Corps of Engineers, Technical Memo No. 51, 24 p.

6. Brooks, N. H., 1963, Discussion of Proc. Paper 3273, Journal of the Hydraulics Division, Proc., ASCE, Vol. 89, No. HY3, pp 327-333.

7. Chang, Y. L., 1939, Laboratory Investigation of Flume Traction and Transportation, Trans., ASCE, Vol. 104, Paper 2037, p. 1274.

8. 1968, Colorado State University, Civil Engineering Department, Scour Study Data, Reported by Opie, T. R., 1967, Scour at Culvert Outlets, M.S. Thesis, Colorado State University, Fort Collins, Colorado, 82 p.

9. Eagleson, P. S., Peralta, L. A., and Dean, R. G., 1958, The Mechanics of the Motion of Discrete Spherical Bottom Sediment Particles Due to Shoaling Waves, Beach Erosion Board, Corps of Engineers, Tech. Memo No. 104, 41 p., Appendix.

10. Einstein, H. A., 1942, Formulas for the Transportation of Bed Load, Trans., ASCE, Vol. 107, pp. 561-577.

11. Einstein, H. A., and El-Sami El-Sayed Ahmed, 1949, Hydrodynamic Forces on a Rough Wall, Review of Modern Physics, Vol. 21, No. 3, pp. 520-524.

12. Gessler, J., 1965, The Beginning of Bed Load Movement of Mixtures Investigated as Natural Armoring in Channels, Lab of Hydraulic Research and Soil Mechanics, Swiss Federal Institute of Tech., Zurich, Report No. 69, Translated by Prych, E. A., 1967, W. M. Keck Lab of Hydraulics and Water Resources, California Institute of Technology, Pasadena, California.

13. Iwagaki, Y., 1956, Hydrodynamical Study on Critical Tractive Force, Trans., Japanese Society of Civil Engineers, No. 41, After Garde and Hasan (1967), Ref. (3).

REFERENCES - Continued

14. Kalinske, A. A., 1942, The Role of Turbulence in River Hydraulics, Proc. of the Second Hydraulics Conference, University of Iowa, Iowa City, Iowa, pp. 266-279.

15. Kellerhals, R., 1963, Gravel Rivers with Low Sediment Charge, Master's Thesis, University of Alberta, Edmonton, Alberta, Canada.

16. Lane, E. W., and Carlson, E. J., 1953, Some Factors Affecting the Stability of Canals Constructed in Coarse Granular Materials, Proc., Minnesota International Hydraulics Convention, pp. 37-48.

17. Leliavsky, S., 1959, An Introduction to Fluvial Hydraulics, Second Edition, Constable and Co., Ltd., London, 257 p.

18. Mavis, F. T., and Tu, Yun-Cheng, 1935, The Transportation of Detritus by Flowing Water-I, University of Iowa Studies, Studies in Engineering Bulletin 5, 53 p.

19. McQuivey, R. S., 1967, Turbulence in a Hydrodynamically Rough and Smooth Open Channel Flow, Ph.D. Dissertation, Colorado State University, Fort Collins, Colorado, 105 p.

20. Prus-Chacinski, T. M., 1966, Discussion of Proceedings Paper No. 4387, ASCE, Vol. 92, No. HY2, pp. 389-393.

21. 1943, Punjab Research Institute, Report for the year ending April, 1941, Lahore, Punjab, Superintendent of Government Printing, After Simons (1957).

22. Reid, R. O., 1957, Modification of the Quadratic Bottom-Stress Law for Turbulent Channel Flow in the Presence of Surface Wind-Stress, Beach Erosion Board, Corps of Engineers, Tech. Memo No. 93, 33 p., Appendix.

23. Rozovskii, I. L., 1957, Flow of Water in Bends of Open Channels, Academy of Sciences, Ukranian S.S.R., Kiev, U.S.S.R. Translated from Russian, Published for the National Science Foundation, Washington, D. C., and the Department of the Interior by the Israel Program for Scientific Translation, 233 p.

24. Saville, T., Jr., 1954, The Effect of Fetch Width on Wave Generation, Beach Erosion Board, Corps of Engineers, Tech. Memo No. 70, 9 p.

25. Sibul, O., 1955, Laboratory Study of the Generation of Wind Waves in Shallow Water, Beach Erosion Board, Corps of Engineers Tech. Memo No. 72, 35 p.

26. Simons, D. B., and Richardson, E. V., 1964, Resistance to Flow in Alluvial Channels, Colorado State University, Department of Civil Engineering, Civil Engineering Report, CER64-DBS-EVR8, p. 176, Figures and Tables.

27. Simons, D. B., 1957, Theory and Design of Stable Channels in Alluvial Materials, Ph.D. Dissertation, Colorado State University, Fort Collins, Colorado, 394 p.

REFERENCES - Continued

28. State of California, 1960, Bank and Shore Protection in California
     Highway Practice, Department of Public Works, Division of Highways,
     Sacramento, California, 423 p.

29. 1948, The Central Board of Irrigation Journal, India, Annual Report,
     Part I., pp. 253-261 and also p. 74 of 1943 Journal.

30. Thomson, S. M., 1965, The Transport of Gravel by Rivers, Proc. of
     the Second Australasian Conference on Hydraulics and Fluid Mechanics,
     New Zealand, pp. A259-A274.

31. Torum, A., 1965, Stability of Gravel Mound Exposed to Simultaneous
     Action of Waves and Currents, XI Congress, International Association
     for Hydraulic Research, Leningrad, 9 p.

32. 1935, U. S. Waterways Experiment Station, Vicksburg, Mississippi,
     Paper 17, Studies of River Bed Materials and Their Movement, with
     Special Reference to the Lower Mississippi River, pp. 57-86.

33. 1958, Velocity Forces on Submerged Rocks, U. S. Army Engineer Water-
     ways Experiment Station, Corps of Engineers, Waterways Experiment
     Station Miscellaneous Paper No. 2-265, Vicksburg, Mississippi,
     Plate 1.

34. Urbonas, B. R., 1968, Forces on a Bed Particle in a Dumped Rock
     Silting Basin, Master's Thesis, Colorado State University, Fort
     Collins, Colorado, 69 p.

APPENDIX II. - LIST OF SELECTED SYMBOLS

A	Area
C	Chezy's coefficient
C_D	Drag force coefficient
C_L	Lift force coefficient
D	Depth of flow
$\bar{D}$	Average depth of flow
$Dmax$	Maximum depth of flow
D_b	Bottom depth of flow
d	Diameter of a sphere
d_s	Diameter of riprap particles
d_{50}	Sieve diameter when 50 percent are finer
d_{75}	Sieve diameter when 75 percent are finer
d_{85}	Sieve diameter when 85 percent are finer
F	Fetch length
F_b	Free board
F_e	Effective fetch length
F_D	Drag force
F_{Db}	Drag force on bed
F_{DS}	Drag force on sloping bank
F_L	Lift force
F_p	Pressure force
Fr	Froude number
f_s	Seepage force
g	Acceleration due to gravity
H	Depth of flow

H_s	Significant wave height
n	Manning's roughness coefficient
Q	Total discharge
R	Hydraulic radius
R_e	Resultant forces
$\mathbb{R}$	Reynolds number
$\mathbb{R}_p$	Particle Reynolds number
$\mathbb{R}_*$	Shear Reynolds number
r_c	Radius of curvature of center line of bends
r_i	Radius of curvature of inner bank of bends
r_o	Radius of curvature of outer bank of bends
Se	Energy grade line
S_s	Specific gravity of the solids
T	Wave period
T_c	Shield's parameter
$\overline{V}$	Average velocity
$Vmax$	Maximum velocity
V_b	Bottom velocity
V_s	Seepage velocity
V_*	Shear velocity
V_w	Wind velocity
V_{we}	Effective wind velocity
V_{wm}	Maximum wave velocity
W_T	Water surface width
ΔZ	Superelevation

α	Angle of bank with horizontal
α_1	Angle between direction of flow and axis of channel
α'	Slope of the bed
γ	Specific weight of water
γ_s	Specific weight of solid
Δ°	Central deflection angle of bend
Δ'	$0.42\Delta \, (D_{max}/W_T) \, \sqrt{g}/C$
ΔD	Depth correction
η	Stability coefficient
$\oplus$	Direction of wind with channel axis
ν	Kinematic viscosity
ρ_f	Density of fluid
ρ_s	Density of solid
τ_o	Average bottom shear stress
τ_t	Total shear stress
τ_c	Critical shear stress
τ_s	Shear stress on sides
τ_{sd}	Design shear stress on sides
ϕ	Angle of repose
$1/\psi$	Lift force factor

APPENDIX III
FIGURES

Flow Velocity , V in fps

△ Indri Graded Particle V=Q/A put to motion	◐ Schaffemak Begining of motion V = Q/A
◇ Meyer Peter and Muller Uniform particle in motion Q/A	◑ " Grains kept in motion Q/A
▽ " " Uniform broken particle put in motion Q/A	◒ Vibrating and oscillating Q/A
◓ CSU Data Graded material 0.25 ft above bottom	∅ Ho's 0.25 ft above bed
● Lane Q/A	⊖ " Uniform 0.05 ft above bed
▣ Bhowmik and Wend (inside) 0.5 ft above bottom	⊕ Tu's particles put to motion 0.25 ft. above bed
▲ Linnton Hydraulic Lab (gravel)	⊕ " 0.05 ft above bed
○ Kellerhas Q/A	

Isolated Cubes $W_o = 2.42\,dn$, W_o = fall velocity for natural particle, $S_f = 0.7$

Smith and Hallmark

Stilling Basin (USBR)

ISBASH

Design Curve

Mean Particle Diameter in inches

Fig. 1.   Relation Between Velocity and Mean Particle Diameter
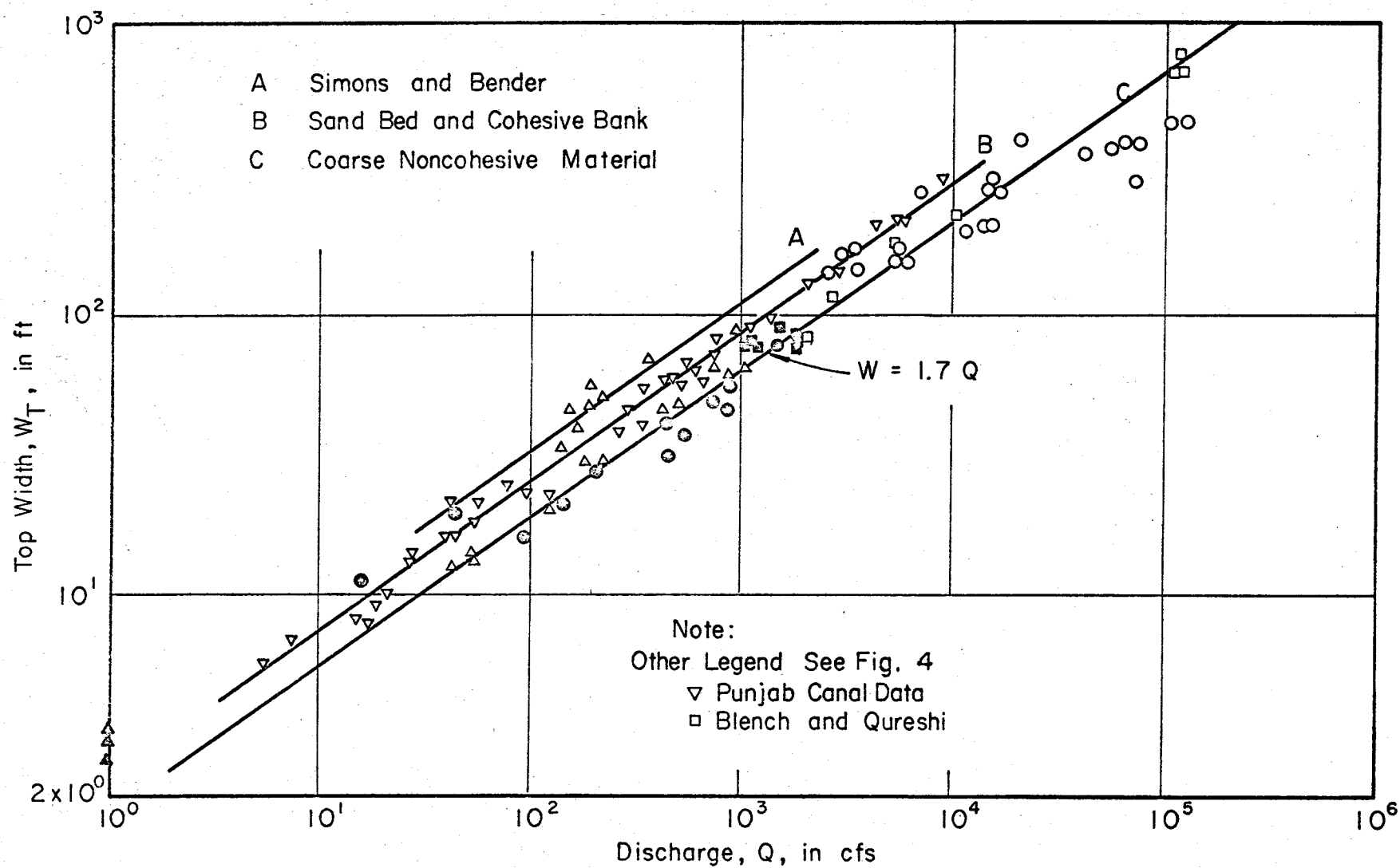
Fig. 2. Relation Between Top Width, W_T, and Discharge, Q
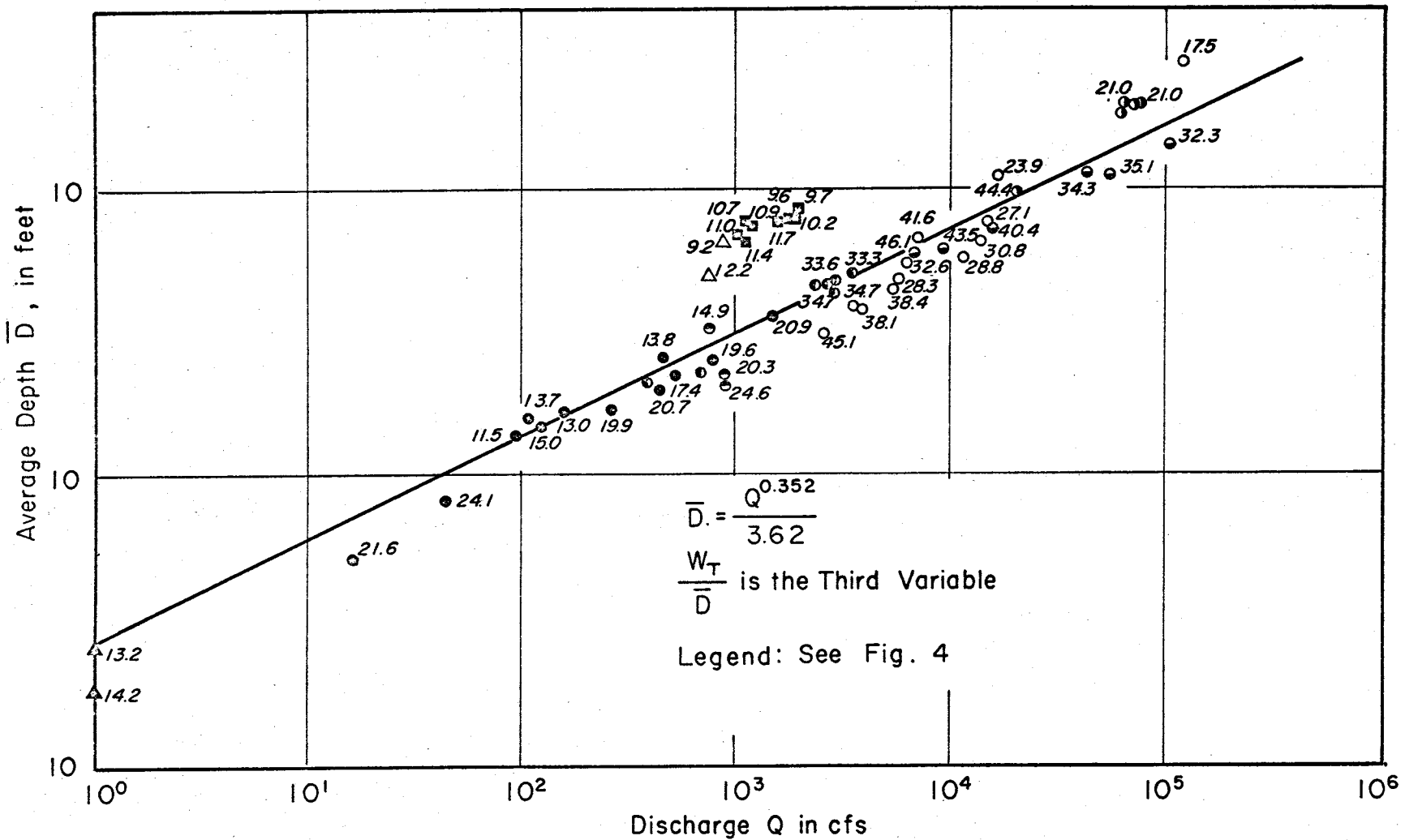
Fig. 3. Relation Between Average Depth and Discharge, Q

$$\overline{D}. = \frac{Q^{0.352}}{3.62}$$

$\dfrac{W_T}{\overline{D}}$ is the Third Variable

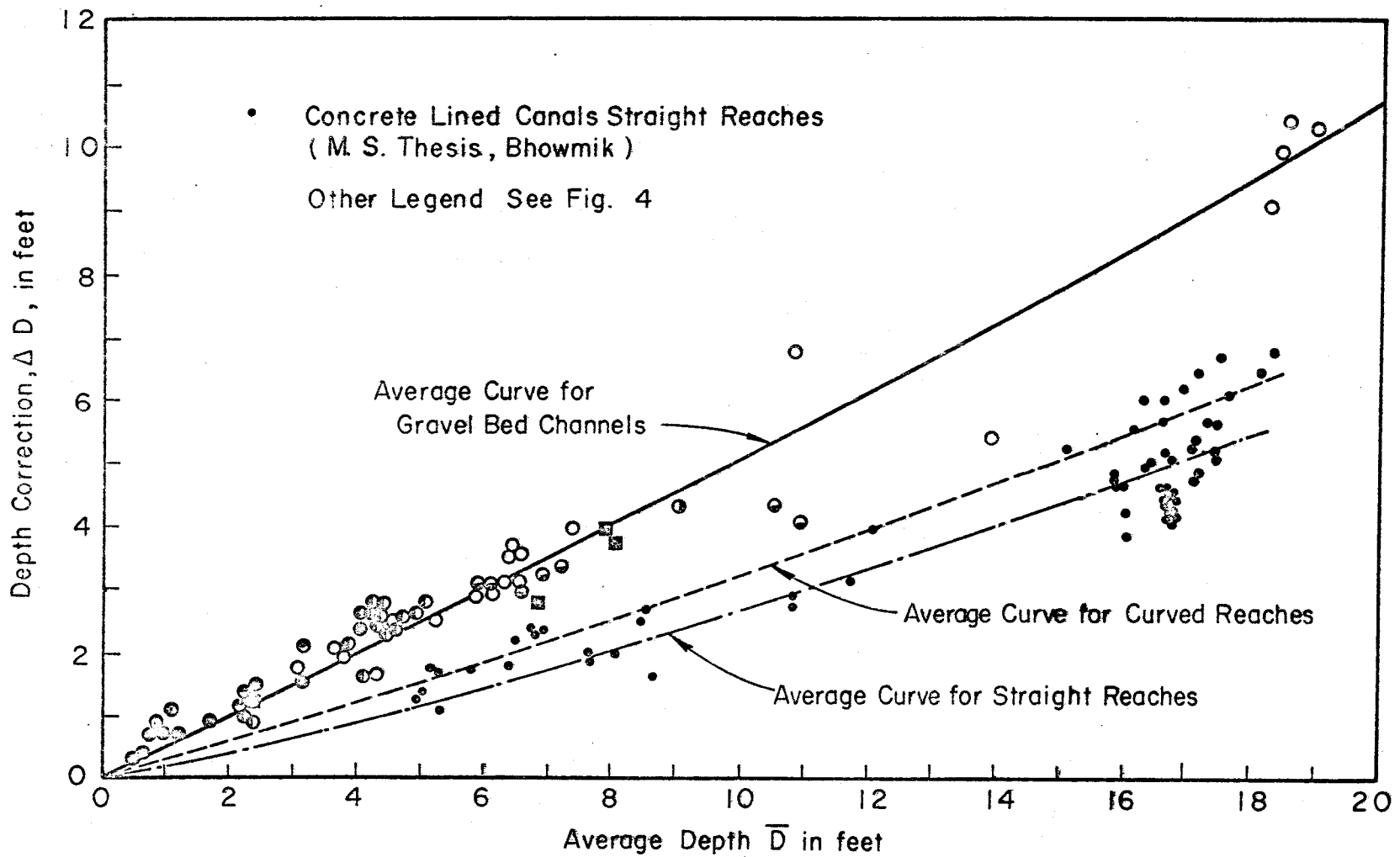Legend: See Fig. 4
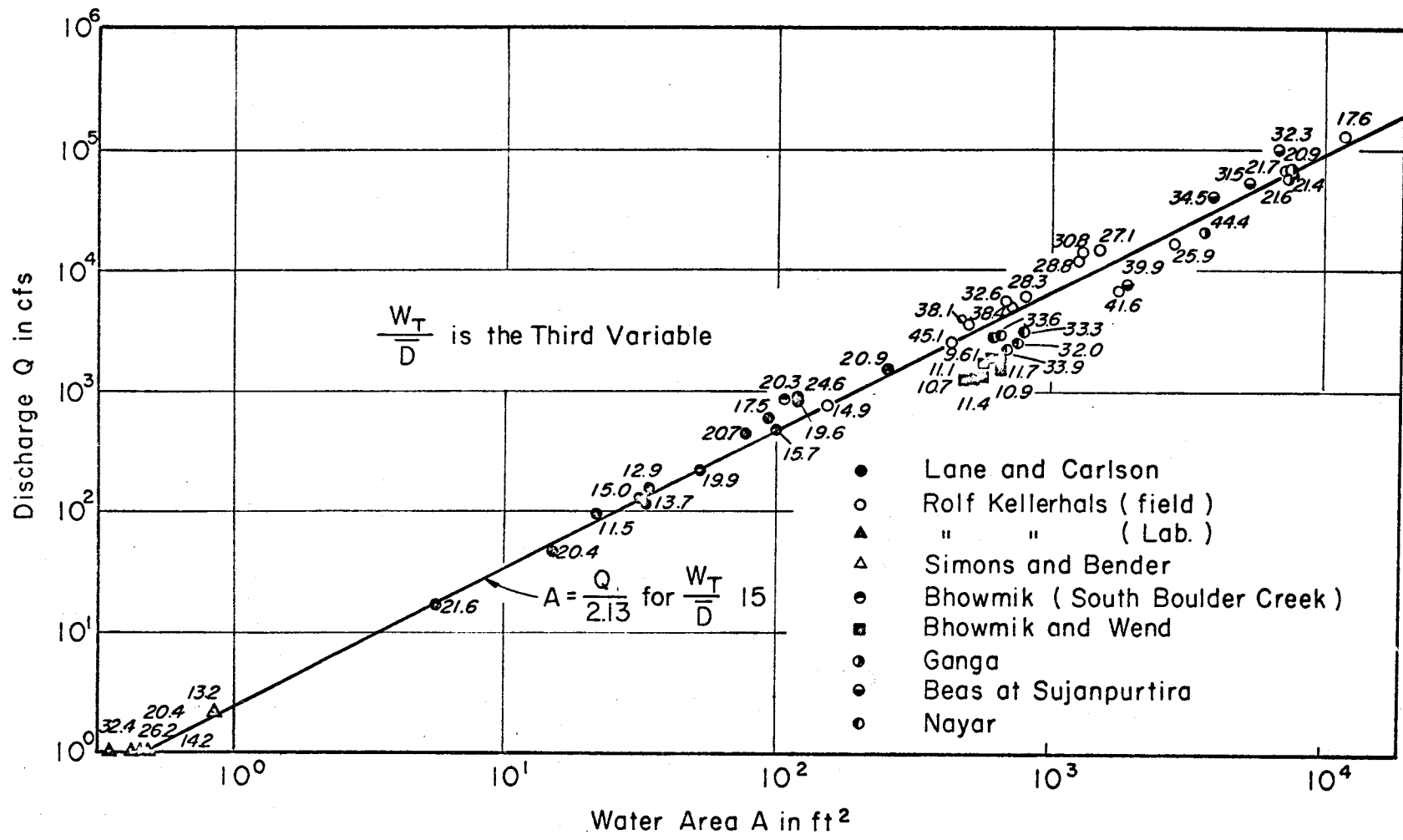
Fig. 4. Relation Between Water Area, A, and Discharge, Q

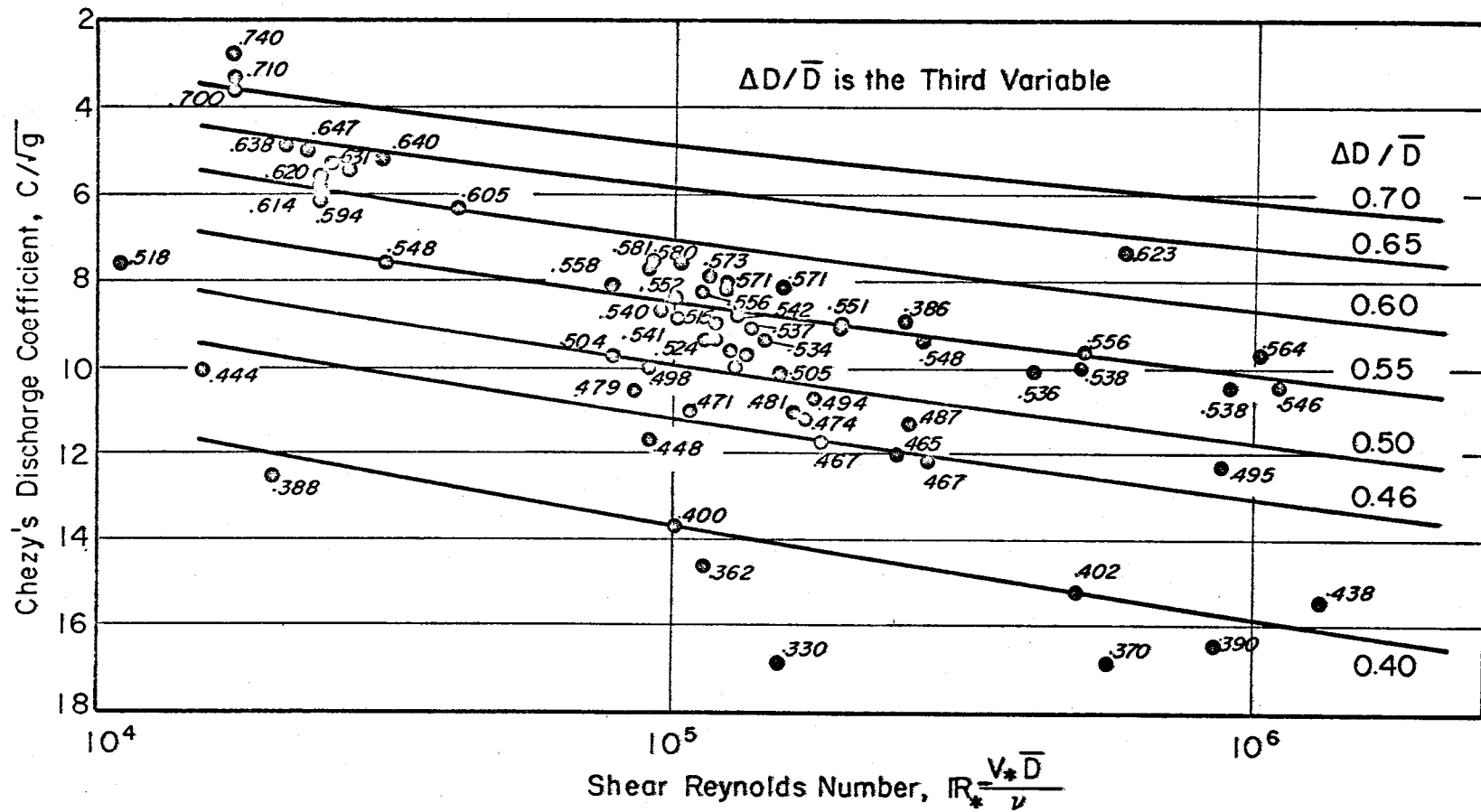Fig. 5. Relation Between Depth Correction, ΔD, and Average Depth, $\overline{D}$

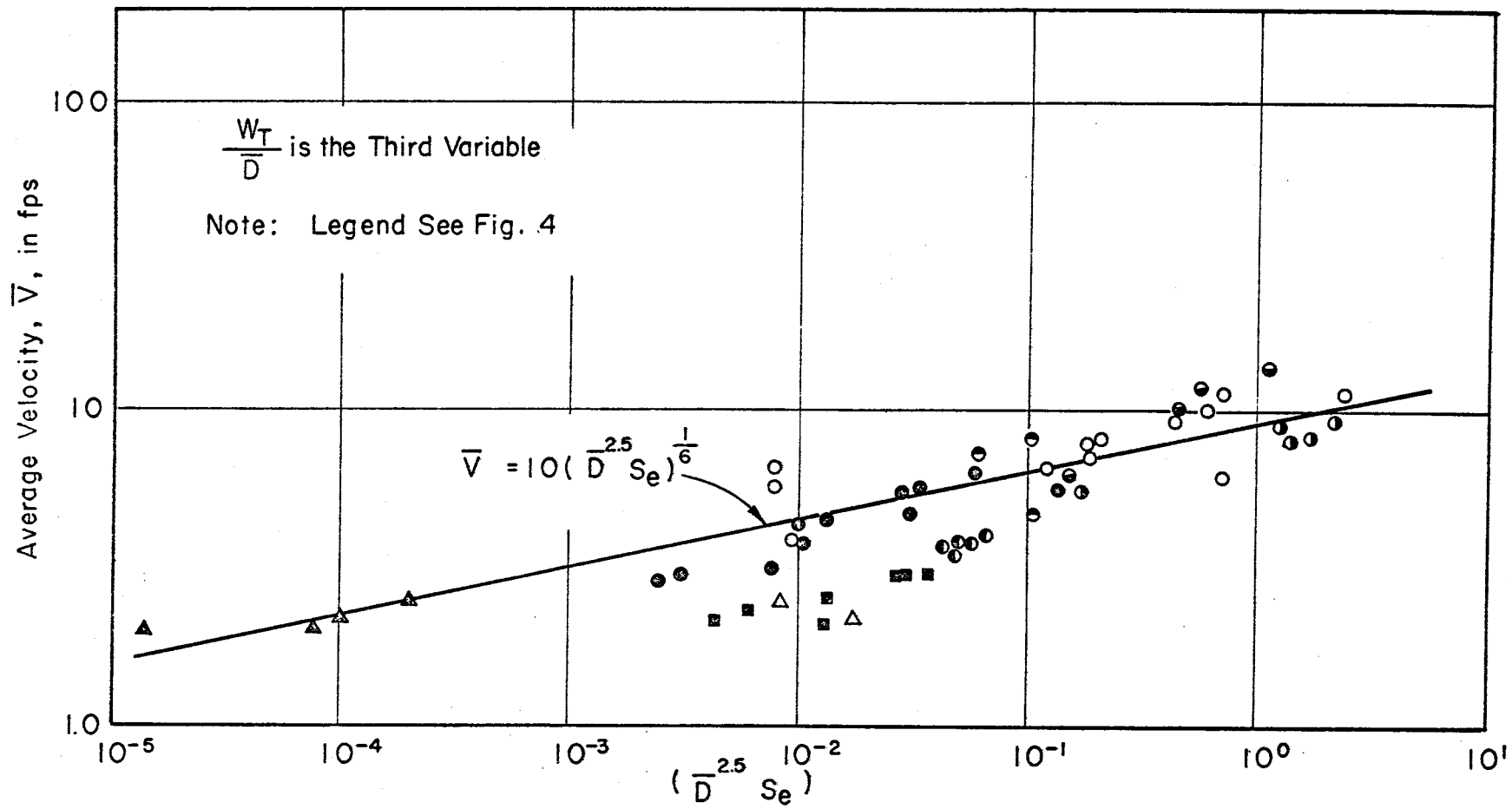Fig. 6. Resistance Diagram Relating $C/\sqrt{g}$, $\mathbb{R}_*$ and $(\Delta D/\overline{D})$

Fig. 7. Relation Between Average Velocity $\overline{V}$ and $(\overline{D}^{2.5} S_e)$
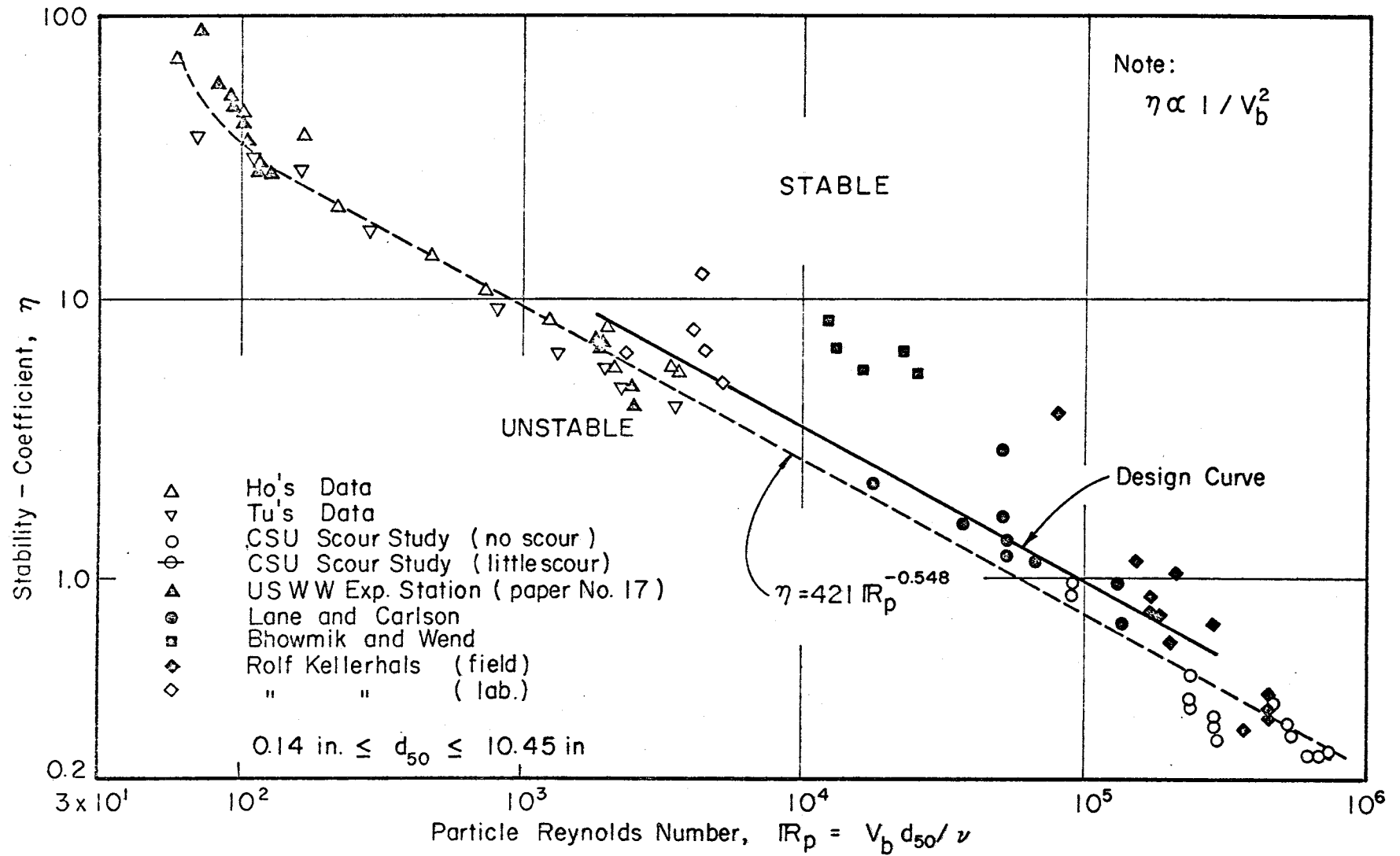
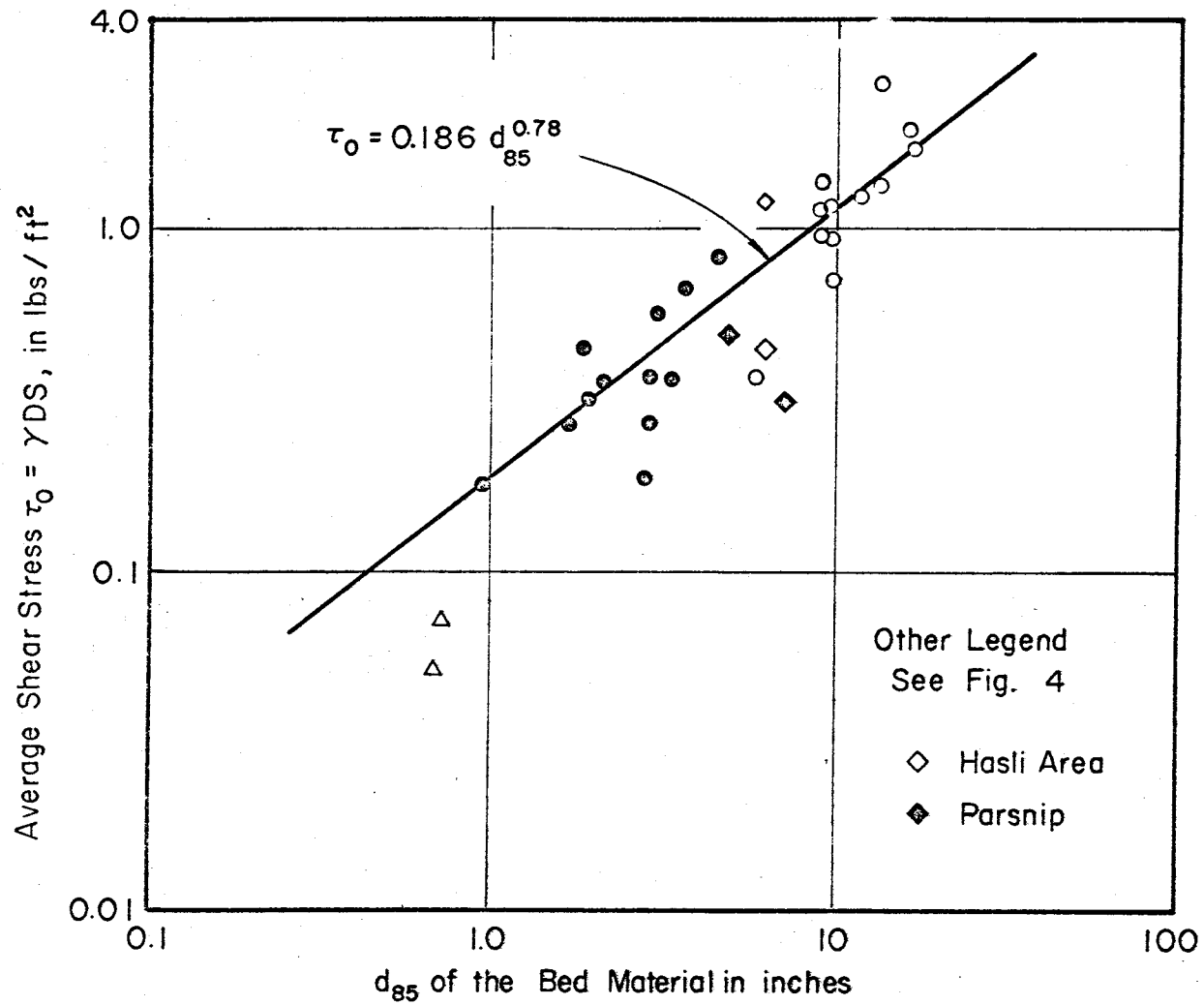Fig. 8. Stability Coefficient, η, and Particle Reynolds Number

Note:
$$\eta \propto 1 / V_b^2$$

STABLE

UNSTABLE

Stability – Coefficient, η

Particle Reynolds Number, $\mathbb{R}_p = V_b d_{50} / \nu$

$\triangle$ Ho's   Data
$\triangledown$ Tu's   Data
$\circ$ CSU   Scour Study   (no scour)
ϕ CSU   Scour Study   (little scour)
$\triangle$ US W W Exp. Station (paper No. 17)
$\oplus$ Lane and Carlson
$\blacksquare$ Bhowmik and Wend
$\diamondsuit$ Rolf Kellerhals   (field)
$\diamondsuit$ "   "   (lab.)

0.14 in. $\leq$ d_{50} $\leq$ 10.45 in

$\eta = 421 \, \mathbb{R}_p^{-0.548}$

Design Curve

Fig. 9. Relation Between Average Shear Stress and d_{85} Size of the Bed Material

The figure shows a log-log plot with the y-axis labeled "Average Shear Stress $\tau_0 = \gamma DS$, in lbs/ft^2" ranging from 0.01 to 4.0, and the x-axis labeled "d_{85} of the Bed Material in inches" ranging from 0.1 to 100. The equation shown is:

$$\tau_0 = 0.186 \, d_{85}^{0.78}$$

Legend:
Other Legend
See Fig. 4

◇ Hasli Area
◈ Parsnip

6
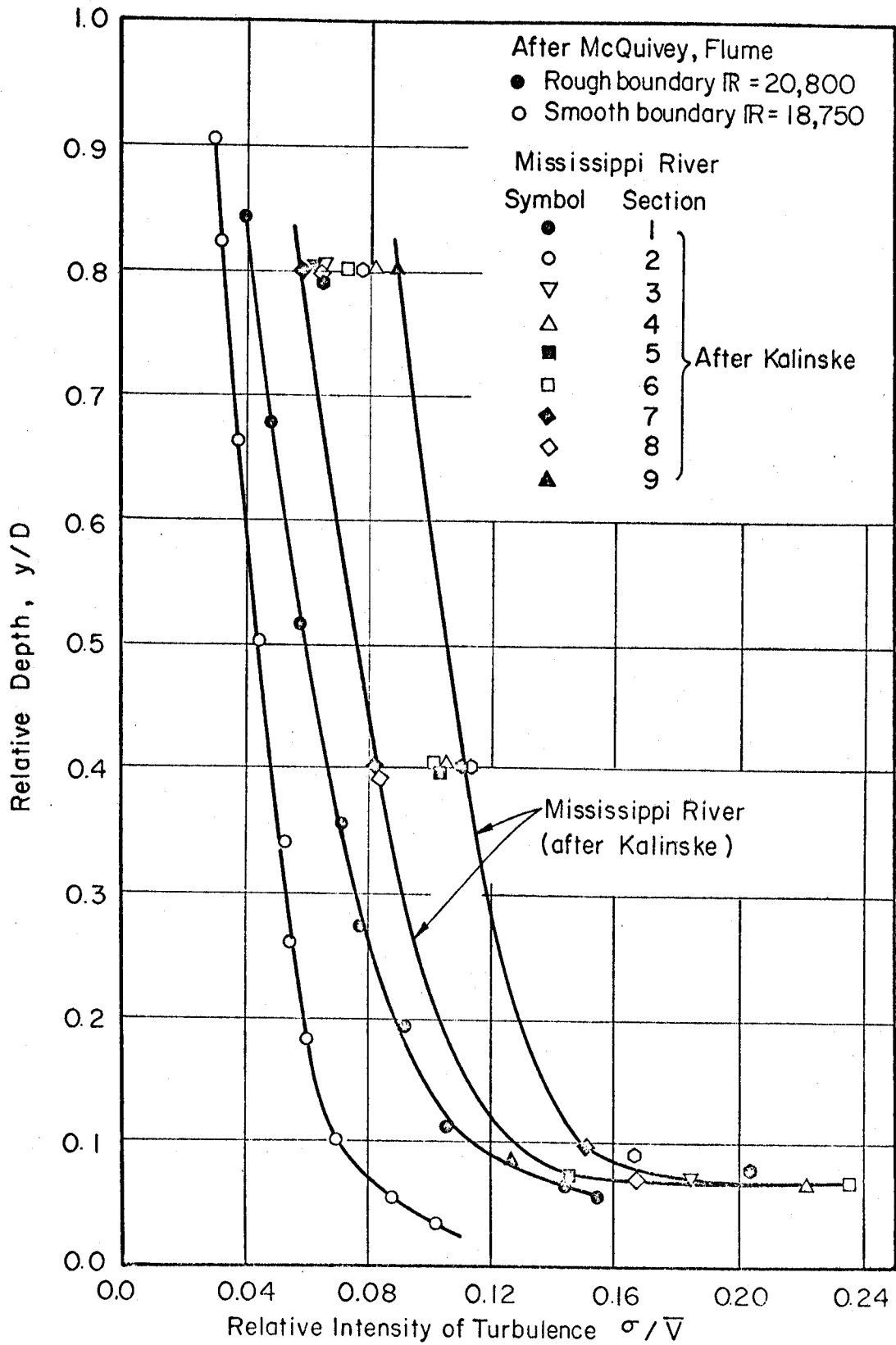
Fig. 10. Turbulent Intensity Distribution For Flume
and The Mississippi River
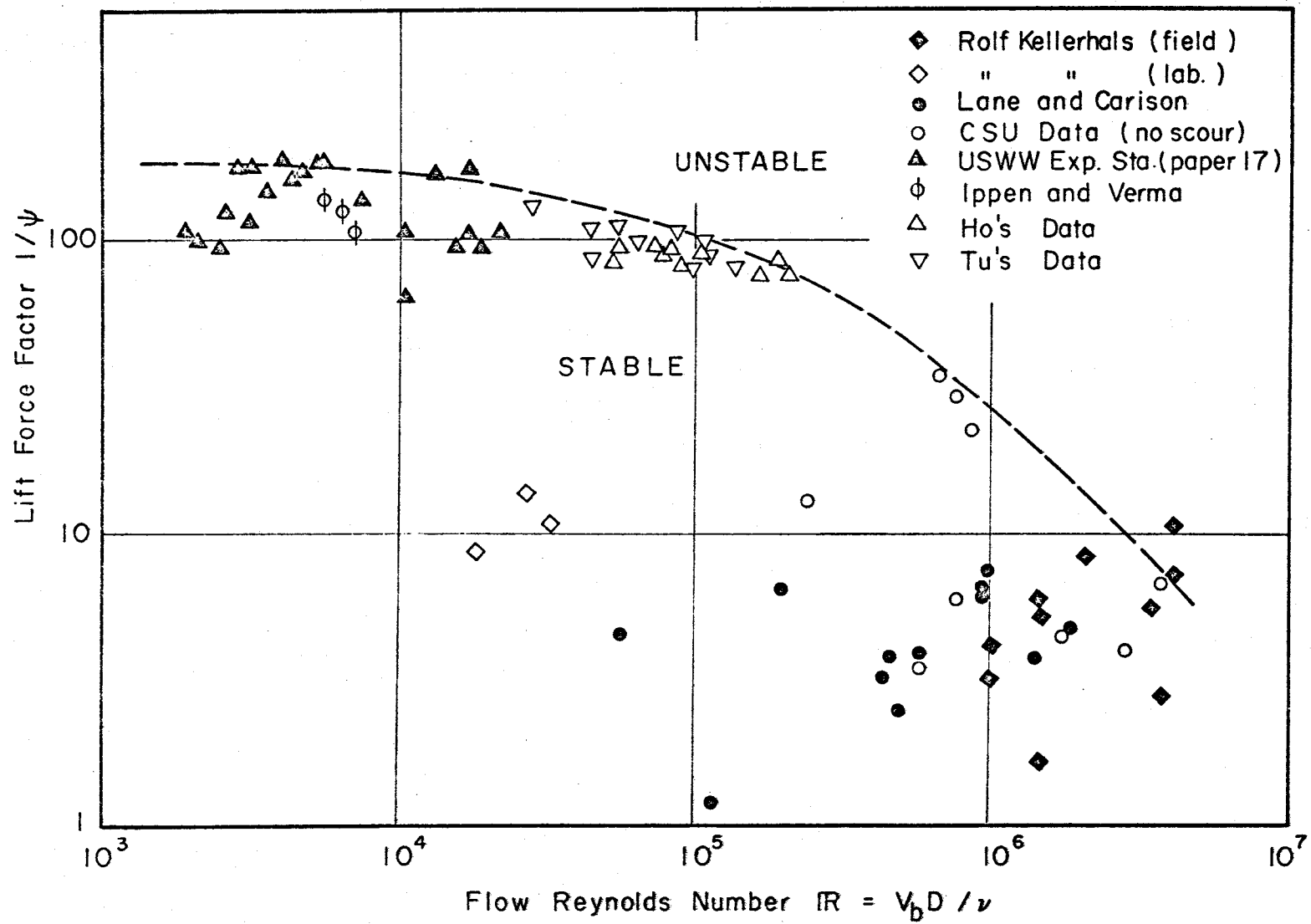
Fig. 11. $\frac{1}{\psi}$ Versus Flow Reynolds Number
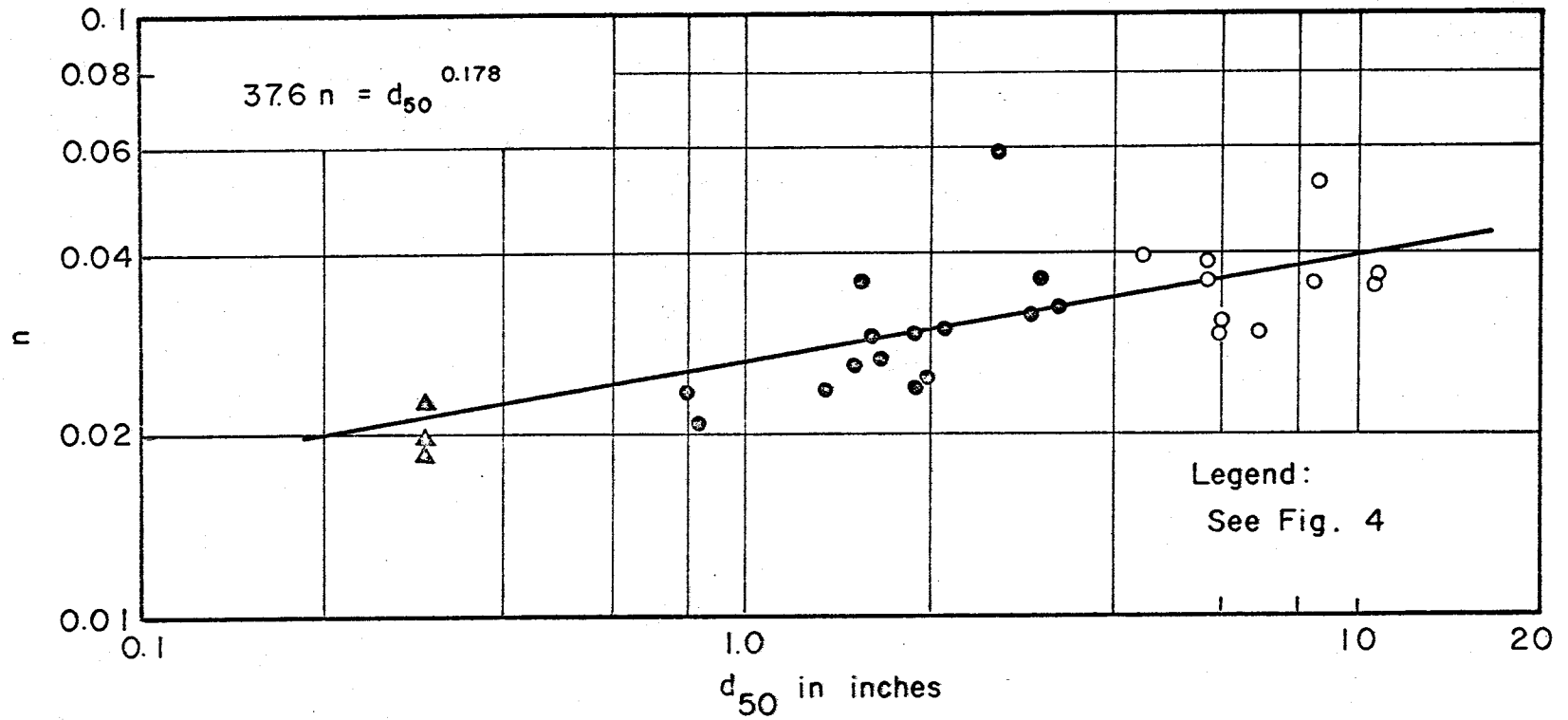
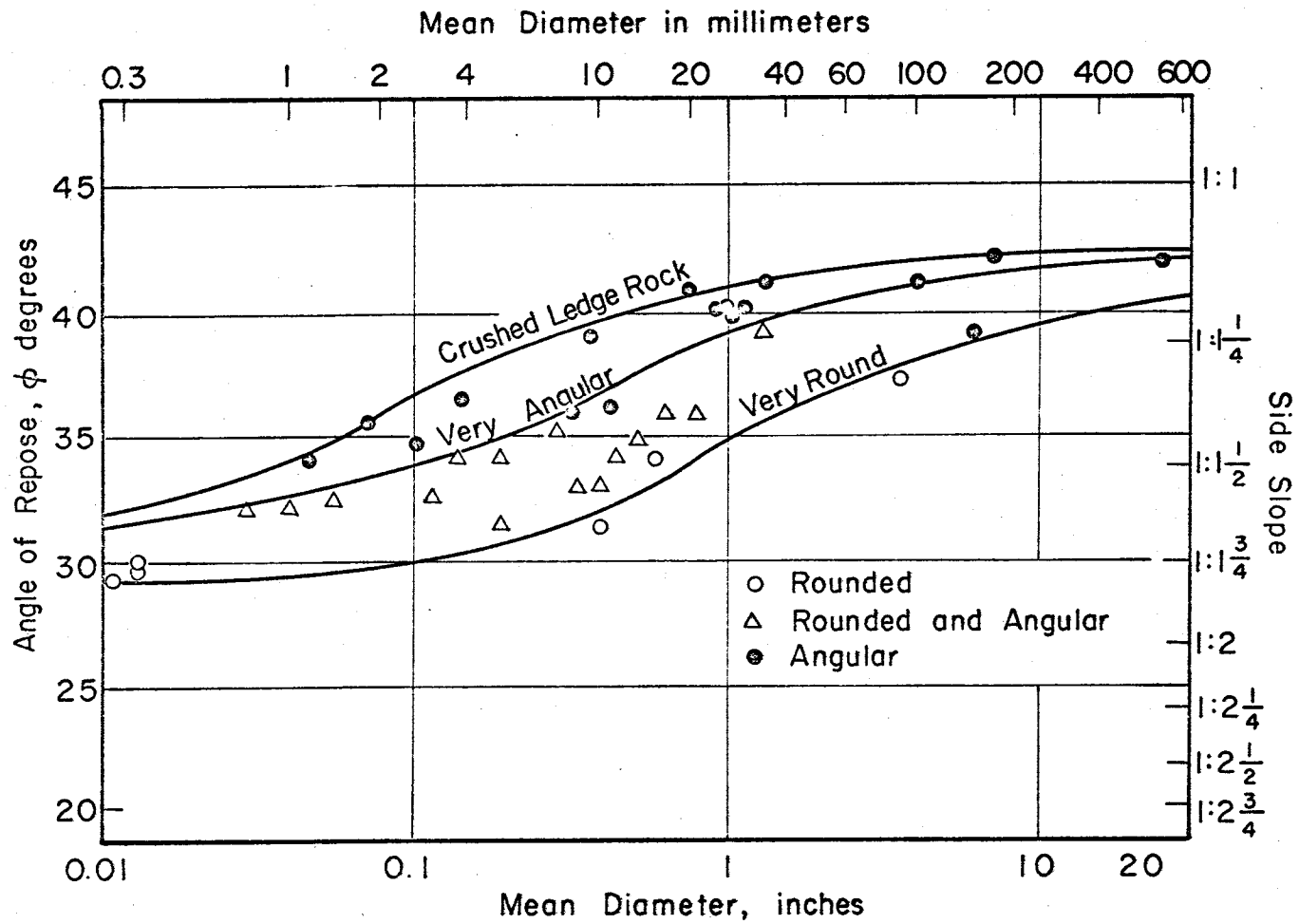Fig. 12. Relation Between Manning' n and Mean Bed Material Diameter

Fig. 13. Angle of Repose of Non-cohesive Material

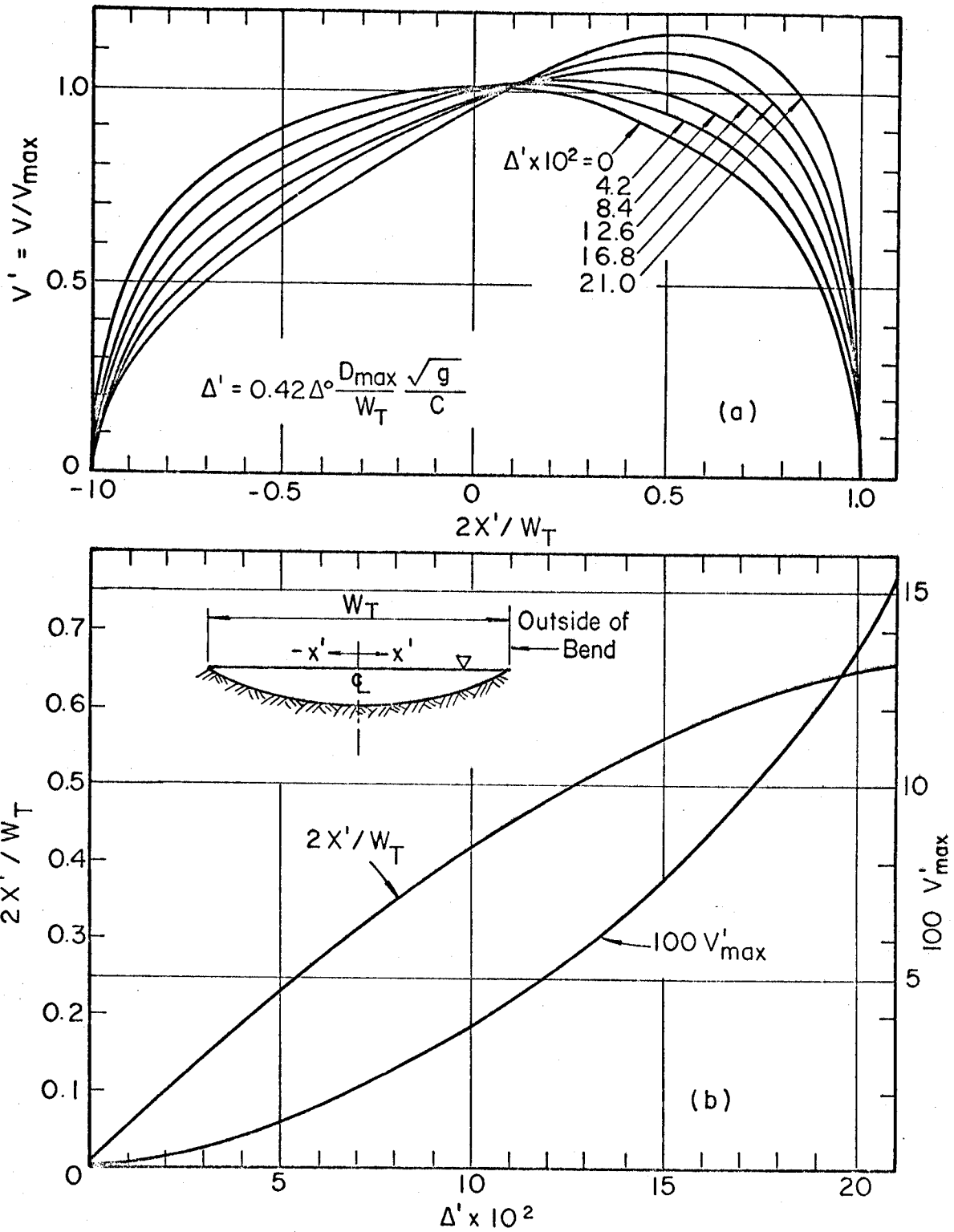$$\Delta' = 0.42\Delta° \frac{D_{max}}{W_T} \frac{\sqrt{g}}{C}$$

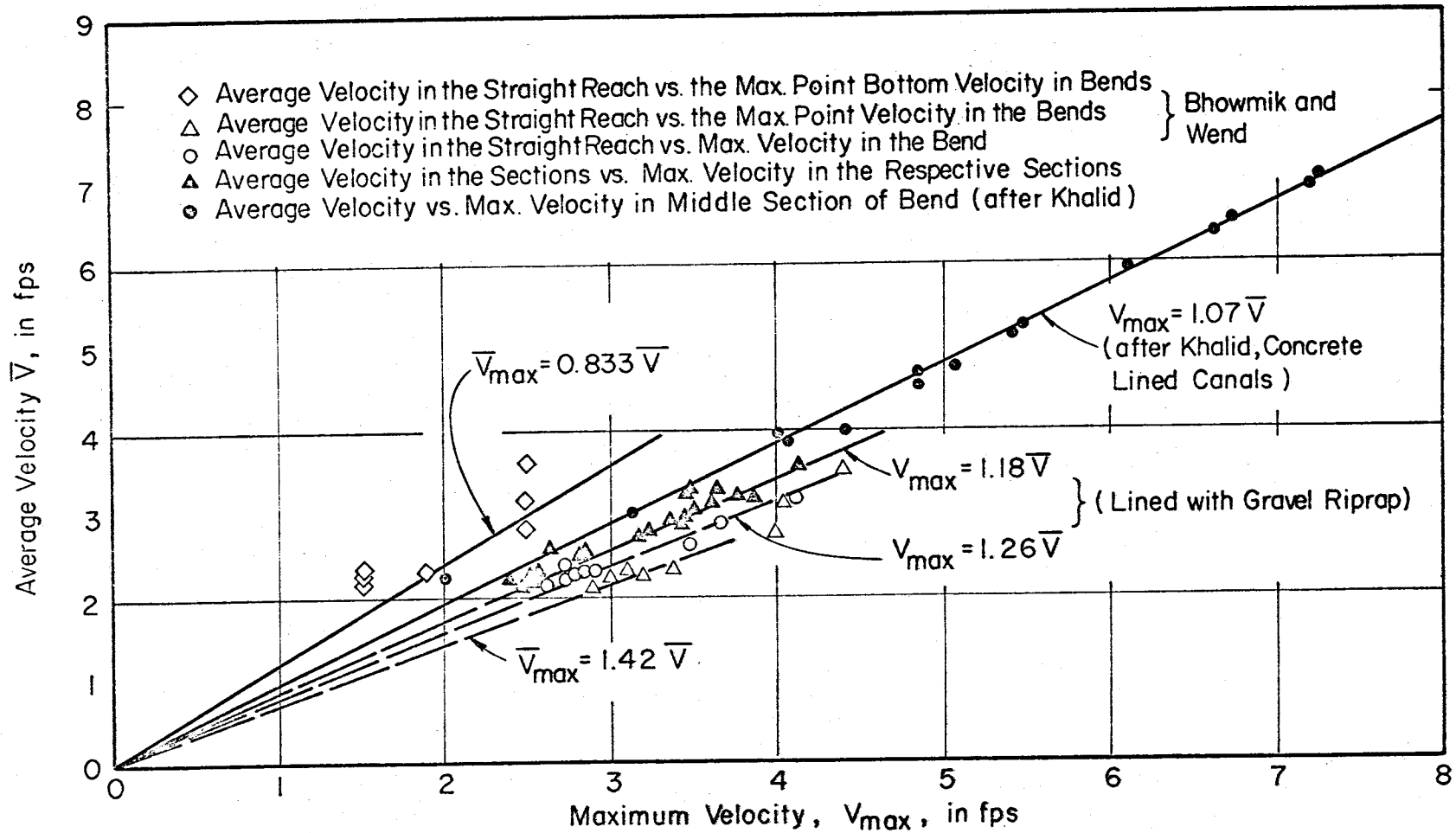(a)

(b)

Fig. 14. Dimensionless Curves For Bend Effects

Fig. 15. Relation Between the Average Velocity and the Maximum Velocity in the Bends
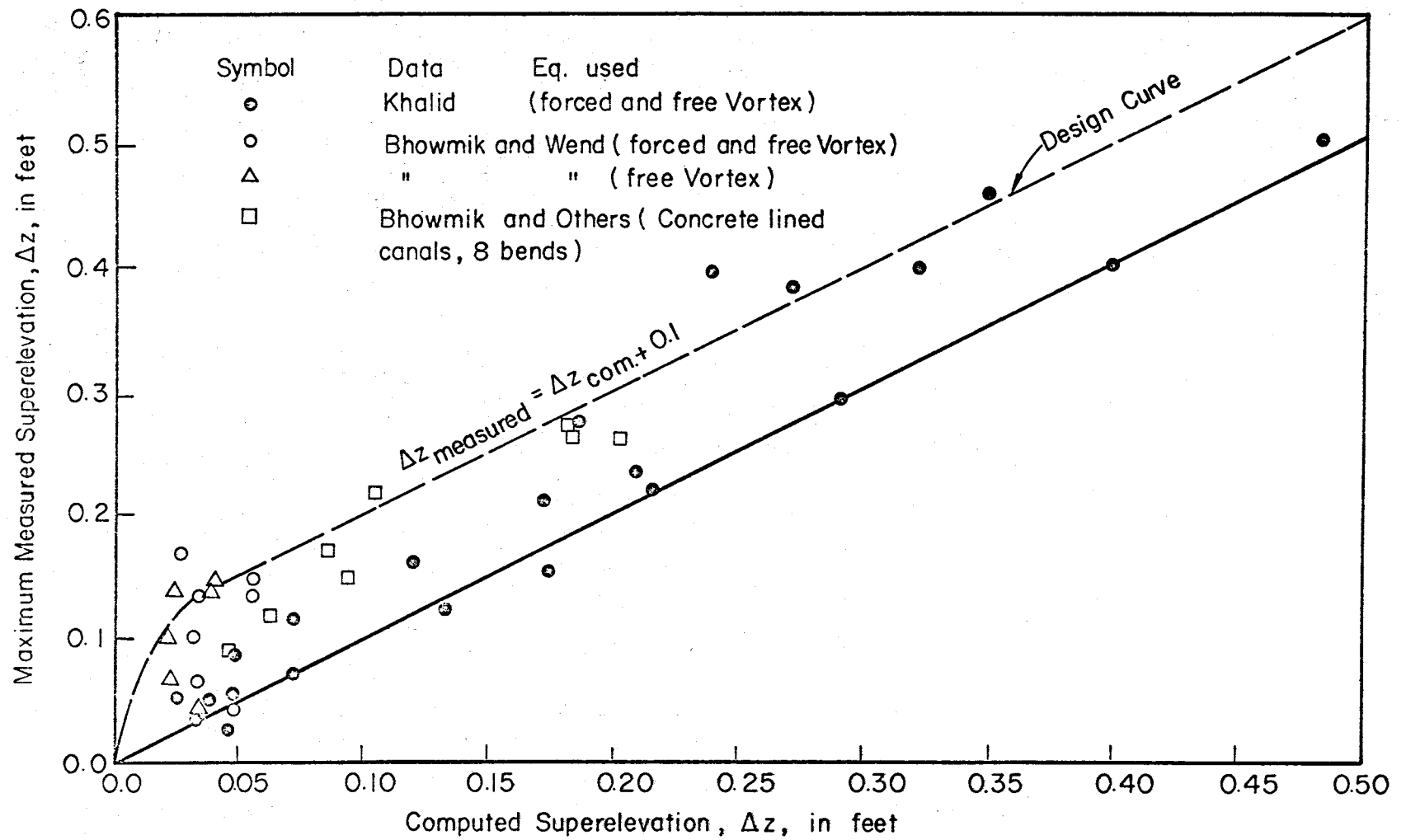
Fig. 16. Relation Between the Maximum Measured and Computed Superelevation

Publications:

Assifi, Abdul T., Hydraulics and geometry of rivers, M.S. thesis,
    Colorado State University, 1966, 80 p.

Bhowmik, N.D., The mechanics of flow and stability of alluvial channels
    formed in coarse materials, Ph.D. Dissertation, August 1968.   230 pp